Journal of Biomolecular NMR, **17:** 33–42, 2000.
KLUWER/ESCOM

Deuterium isotope effects on the central carbon metabolism of *Escherichia coli* cells grown on a D_2O-containing minimal medium

Michel Hochuli, Thomas Szyperski* & Kurt Wüthrich**
Institut für Molekularbiologie und Biophysik, Eidgenössische Technische Hochschule Hönggerberg, CH-8093 Zürich, Switzerland

Received 7 September 1999; Accepted 28 February 2000

Key words: biosynthetic fractional ^{13}C-labeling, central carbon metabolism, deuterium isotope effects, protein deuteration

Abstract

Isotope effects on the central carbon metabolism due to the addition of variable amounts of D_2O (0 to 70%) were investigated with biosynthetically directed fractional ^{13}C-labeling for *Escherichia coli* BL21(DE3) cells during exponential growth on a M9 minimal medium containing a mixture of 70% unlabeled and 30% uniformly ^{13}C-labeled glucose as the sole carbon source. The resulting ^{13}C-labeling patterns in the amino acids were analysed by two-dimensional [^{13}C,^{1}H]-correlation spectroscopy. With the aforementioned growth conditions, higher D_2O contents resulted in an increase of the anaplerotic supply of the tricarboxylic acid cycle via carboxylation of phosphoenolpyruvate when compared to the influx of acetyl-CoA. Furthermore, the addition of D_2O affected the C_1 metabolic pathways that involve Ser and Gly. Otherwise the *E. coli* cells showed identical topologies of the active biosynthetic pathways in H_2O and at elevated D_2O contents, and the metabolic flux ratios characterizing glycolysis and the pentose phosphate pathway were not measurably affected by the addition of D_2O. Cells that had been adapted for growth in D_2O exhibited the same response to the presence of D_2O in the nutrient medium as non-adapted cells. Implications of these data for the preparation of recombinant deuterated proteins for NMR studies are discussed.

Abbreviations: DSS, 2,2-dimethyl-2-silapentane-5-sulfonate; HSQC, heteronuclear single-quantum coherence; INEPT, insensitive nuclei enhanced by polarization transfer; TOCSY, total correlation spectroscopy; 2D, two-dimensional; CoA, coenzyme A; TCA, tricarboxylic acid cycle. Additional symbols for intermediary metabolites are explained in Table 1 and Figure 4.

Introduction

For NMR applications in structural biology, efficient production of uniformly or partially deuterium-labeled proteins is of keen interest (LeMaster, 1994; Gardner and Kay, 1998). Deuterium-labeled proteins are commonly expressed in bacteria growing on media containing D_2O and either protonated or deuterated carbon sources, depending on the desired pattern of deuterium incorporation (Gardner and Kay, 1998). It has long been known that, although nutrient media containing sizeable fractions of D_2O are tolerated by many bacteria and lower eucaryotes, a reduction of the growth rate and lower biomass yields are generally observed in D_2O-containing media (Katz and Crespi, 1970). Such effects of deuterium on biological systems may be due to isotope effects from the solvent D_2O and from the replacement of hydrogen with

*Present address: State University of New York at Buffalo, Dept. of Chemistry, Natural Sciences and Mathematics Complex, Buffalo, NY 14260, U.S.A.
**To whom correspondence should be addressed.
Fax no.: +41-1-633 1151.
Supplementary material, available from the authors on request: one Table, listing relative abundance of intact C_2 and C_3 fragments in the amino acids from cultivations in M9 minimal media with 0, 30, 50 and 70% D_2O.

deuterium in the C-H bonds of organic compounds. Deuterium isotope effects are known to influence, for example, the rates of enzyme-catalyzed reactions, ionic equilibria, the strength of hydrogen bonds and the global stability of folded proteins, which may in turn influence allosteric properties of enzymes and genetic control mechanisms (Saur et al., 1968a, b; Katz and Crespi, 1970; Schowen, 1977; Schowen and Schowen, 1982). In this paper we investigate the regulatory response of the central carbon metabolism network in *Escherichia coli* cells to the addition of variable amounts of D_2O to the growth medium.

For the studies of deuterium isotope effects we used the method of biosynthetically directed fractional ^{13}C-labeling combined with 2D [^{13}C,^{1}H]-correlation NMR spectroscopy for the analysis of the resulting nonrandom ^{13}C-labeling patterns in the amino acids (Neri et al., 1989; Senn et al., 1989; Szyperski et al., 1992, 1996, 1999; Szyperski, 1995, 1998; Sauer et al., 1997; Fiaux et al., 1999; Hochuli et al., 1999). In this approach, contiguous carbon fragments from a single carbon source molecule are traced through the cellular bioreaction network. Because the patterns of intact carbon fragments observed for a given metabolite often depend on the specific pathway used for its synthesis, the fractions of molecules that have been synthesized via the different pathways can be quantified. Here, we compare the extent to which the different metabolic pathways are used in the M9 minimal medium either in H_2O or in 70% D_2O/30% H_2O. The *E. coli* strain BL21(DE3) was chosen for this study because it has been frequently used in practice to produce proteins in deuterated media for structural studies (e.g., Venters et al., 1995; Gardner and Kay, 1998).

Materials and methods

Cell growth and sample preparation

Cultures of *E. coli* BL21(DE3) cells (Studier et al., 1990) harbouring the pBR322 plasmid for ampicillin resistance were grown on a series of minimal media which all contained M9 salts (Sambrook et al., 1989), 2 mM $MgSO_4$, 1 μM $FeCl_3$, 1 mg/l each of biotin, choline chloride, folic acid, niacinamide, D-pantothenate and pyridoxal, 0.1 mg/l of riboflavin, 5 mg/l of thiamine, 100 μM $CaCl_2$, 50 μM $ZnSO_4$, 4 g/l of glucose and 50 μg/ml of ampicillin, and differed only by variable D_2O contents from 0 to 70%. For the fractional ^{13}C-labeling, 30% of the glucose, which is the only carbon source in this medium, was uniformly ^{13}C-labeled. For preparations with *E. coli* cells that had not previously been adapted for growth in D_2O-containing media, the above medium containing 0%, 30%, 50% and 70% D_2O was inoculated 1:100 with *E. coli* BL21(DE3) cells from a stationary overnight culture in non-deuterated medium. For preparations with pre-adapted cells, M9 medium containing 70% D_2O was inoculated 1:100 with cells that had been grown to stationary phase successively in M9 media with 0%, 30% and 50% D_2O. The cells were grown in 100 ml batches contained in 1 l Erlenmeyer flasks at 37 °C on a rotary shaker set to 220 rpm. The total culture volume was 2× 100 ml for the non-deuterated medium, 3× 100 ml for the medium with 30% D_2O, 5× 100 ml for the medium with 50% D_2O and 6× 100 ml for the medium with 70% D_2O. Growth was monitored by measuring the optical density at 600 nm (OD_{600}). The cells were harvested at the end of the exponential growth phase. Secreted metabolites in the growth medium were assayed using gas chromatography (5890E, Hewlett-Packard) on a MD-10 column (Macherey and Nagel). The dried biomass was hydrolysed in 6 M hydrochloric acid at 110 °C for 24 h.

The NMR samples were prepared from dried hydrolysate and 20 mM DCl in D_2O, as follows: solvent volume 600 μl; 90, 140, 170 and 170 mg, respectively, of the hydrolysate were dissolved for the cultures grown in H_2O, 30% D_2O/70% H_2O, 50% D_2O/50% H_2O and 70% D_2O/30% H_2O.

NMR experiments and data analysis

For samples obtained from the nutrient medium in H_2O, the ^{13}C-^{13}C scalar coupling fine structures of the amino acids were analysed in 2D [^{13}C,^{1}H]-HSQC spectra (Szyperski et al., 1992). Additional experiments were needed for the samples derived from D_2O-containing cultures, since in 2D [^{13}C,^{1}H]-HSQC-spectra the ^{13}C-^{13}C scalar coupling fine structures of the different deuterium isotopomers are only partially separated by the deuterium isotope effects on the chemical shifts (Hansen, 1988). Many of the ^{13}C fine structures originating from deuterium isotopomers of the aliphatic carbons could be resolved using the following NMR experiments: 2D ^{1}H-TOCSY-relayed [^{13}C,^{1}H]-HSQC (Otting and Wüthrich, 1988); refocused 2D ^{1}H-TOCSY-relayed [^{13}C,^{1}H]-HSQC (Figure 1) with the refocusing INEPT delay tuned to selectively monitor the C-H groups (Burum and Ernst, 1980); 2D [^{13}C,^{1}H]-HSQC with 2.5-fold J-scaling

Table 1. Origin of the intermediates in the central carbon metabolism of *E. coli* BL21(DE3) cells during exponential growth on a M9 minimal medium in H_2O and in 70% D_2O/30% H_2O

Metabolites[a]	Average fraction of total pool (%)[b]	
	H_2O	70% D_2O/30% H_2O[c]
Pentose phosphate pathway		
Pep originating from pentoses	$<23 \pm 5$	$<15 \pm 5$
Ri5P originating from GAP + C_2[d]	70 ± 2	73 ± 2
Ri5P originating from E4P[e]	9 ± 2	7 ± 2
E4P originating from fructose	$>44 \pm 5$	$>44 \pm 5$
Glycolysis		
Pep originating from Oa	5 ± 3	6 ± 4
Pyr originating from malate	0–3	0–4
Tricarboxylic acid cycle		
Oa (*Oa* deuterated at C^3) originating from Pep[f]	36 ± 1	51 ± 3 (27 ± 3)
Oa reversibly interconverted to fumarate	38 ± 10	40 ± 7
Ic originating from glyoxylate and succinate	0–5	0–3
C_1 metabolism		
Ser $C\beta H_2$ (*Ser* $C^\beta HD$) originating from Gly + C_1[g]	28 ± 2	23 ± 3(52 ± 2)
Gly $C^\alpha H_2$ (*Gly* $C^\alpha HD$) originating from CO_2 + C_1[h]	0–3	13 ± 3 (0–3)

[a]Pep, phosphoenolpyruvate; Ri5P, ribose-5-phosphate; GAP, glyceraldehyde-3-phosphate; E4P, erythrose-4-phosphate; Pyr, pyruvate; Oa, oxalacetate; Ic, isocitrate.
[b]The fractions were calculated as described previously (Szyperski, 1995; Sauer et al., 1997). The numbers describe the fraction of the total pool of the metabolite indicated in italics that either originates from the specified pathway or has undergone the specific reversible interconversion reaction. Identical fractions, within the experimental error, were obtained for all cultivations, except for *Oa* originating from Pep and *Gly* $C^\alpha H_2$ originating from CO_2 + C_1 (see text).
[c]The value given is the average obtained from cultivations of non-adapted and D_2O-adapted cells.
[d]Transketolase reaction.
[e]Transketolase and transaldolase reactions.
[f]The data were derived from observation of Asp $C^\beta H_2$, which represents the whole *Oa* pool (see text). The number in parentheses indicates the fraction observed for *Oa* deuterated at C^3, as inferred from Asp $C^\beta HD$ (see text). The corresponding fractions at 30% D_2O and at 50% D_2O were 40 ± 2 (6 ± 2) and 44 ± 2 (17 ± 2).
[g]The number in parentheses indicates the fraction for *Ser* $C^\beta HD$.
[h]The number in parentheses indicates the fraction for *Gly* $C^\alpha HD$.

(Hosur, 1990; Willker et al., 1997). For the aromatic carbons a single ^{13}C fine structure was detected, which could readily be evaluated in the 2D [^{13}C,^1H]-HSQC spectra recorded with the acquisition parameters described in Hochuli et al. (1999). For the 2D ^1H-TOCSY-relayed [^{13}C,^1H]-HSQC spectra and the refocused 2D ^1H-TOCSY-relayed [^{13}C,^1H]-HSQC spectra the ^{13}C-carrier was set to 42.0 ppm relative to DSS. The sweep width was 67.5 ppm and the measurement time was 40 h per spectrum (3000×4096 complex points, $t_{1max} = 353$ ms; $t_{2max} = 682$ ms, 8 scans per t_1 increment, relaxation delay between scans 2 s). For the J-scaled 2D [^{13}C,^1H]-HSQC experiment the ^{13}C-carrier was set to 37.0 ppm relative to DSS and the sweep width was 16.9 ppm. The measurement time was 11 h per spectrum (1500×4096 complex points, $t_{1max} = 353$ ms; $t_{2max} = 614$ ms, 4 scans per t_1 increment, relaxation delay between scans 2 s). All experiments with samples containing partially deuterated amino acids were acquired with deuterium decoupling during t_1 (^{13}C), using WALTZ-16 (Shaka et al., 1983) (see Figure 1). Before Fourier transformation the time domain data were multiplied in t_1 and t_2 with squared sine-bell windows shifted by $\pi/2$ (De Marco and Wüthrich, 1976). The digital resolution after zero-filling was 1.0 Hz/point along ω_1(^{13}C) and 0.7 Hz/point along ω_2(^1H) for the 2D ^1H-TOCSY-relayed [^{13}C,^1H]-HSQC and the refocused 2D ^1H-TOCSY-relayed [^{13}C,^1H]-HSQC spectra, and 1.4 Hz/point along ω_1(^{13}C) and 0.8 Hz/point along ω_2(^1H) for the J-scaled 2D [^{13}C,^1H]-HSQC spectra.

The ^{13}C fine structures were assigned to different sets of deuterium isotopomers based on previously reported deuterium isotope effects on ^{13}C chemical

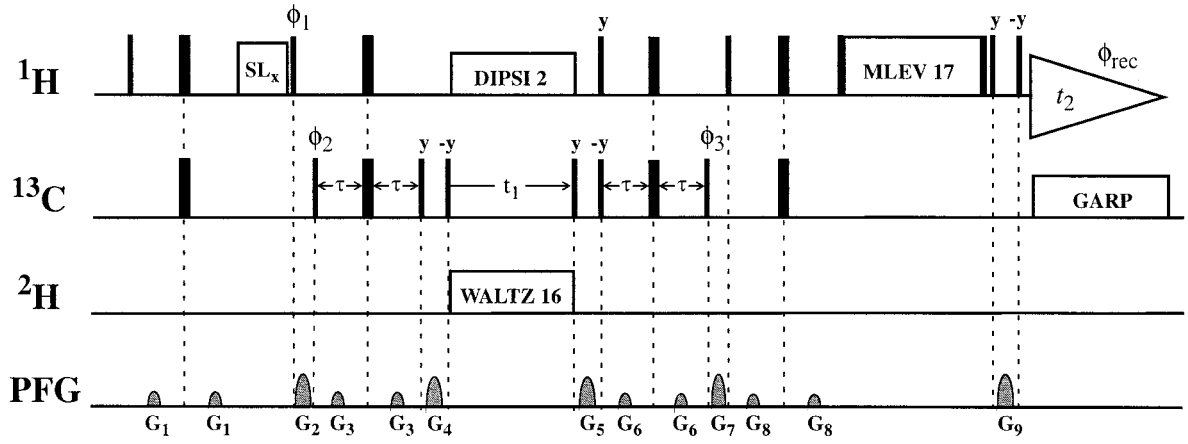

Figure 1. Pulse sequence of the refocused 2D ^{1}H-TOCSY-relayed [^{13}C,^{1}H]-HSQC experiment. The period 2τ in the refocused INEPT is adjusted to $1/(2^1J_{CH})$ for selective observation of C-H groups (Burum and Ernst, 1980). Proton decoupling during t_1 is achieved using the composite pulse decoupling scheme DIPSI-2 (Shaka et al., 1988; Cavanagh and Rance, 1992). z-filters are placed on each side of the t_1 evolution period and before acquisition to obtain pure in-phase ^{13}C-^{13}C scalar coupling fine structures. ^{1}H-TOCSY mixing is performed with the MLEV-17 sequence (Bax and Davis, 1985). The phase cycle is $\phi_1 = \{4y, 4(-y)\}$, $\phi_2 = \{2x, 2(-x)\}$, $\phi_3 = \{x, -x\}$, $\phi_{rec} = \{x, -x, -x, x, -x, x, x, -x\}$, all other pulses x or as indicated. Pulsed field gradients were employed for coherence pathway rejection (Bax and Pochapsky, 1992; Wider and Wüthrich, 1993), and a 2 ms spin-lock pulse was used to purge the magnetization arising from ^{12}C-bound protons and from the residual water signal (Otting and Wüthrich, 1988). ^{13}C-decoupling during t_2 and ^{2}H-decoupling during t_1 were achieved using GARP (Shaka et al., 1985) and WALTZ-16 (Shaka et al., 1983), respectively. Quadrature detection in ω_1 was accomplished with States-TPPI (Marion et al., 1989).

shifts (Hansen, 1988), and on the presence or absence of relay peaks in the 2D ^{1}H-TOCSY-relayed [^{13}C,^{1}H]-HSQC spectra and in the refocused 2D ^{1}H-TOCSY-relayed [^{13}C,^{1}H]-HSQC spectra. The relative abundances of intact carbon fragments in the amino acids originating from a single glucose molecule (*f* values) were calculated from the analysis of the relative multiplet intensities in the ^{13}C-^{13}C scalar coupling fine structures as described by Szyperski (1995), using the program FCAL (Glaser, 1999; Szyperski et al., 1999). Metabolic flux ratios were calculated as described previously (Szyperski, 1995; Szyperski et al., 1996; Sauer et al., 1997).

Results

In an initial phase of this project we investigated some fundamental features of our system in a search of favorable conditions for the subsequent systematic measurements. A first series of labeling experiments with *E. coli* BL21(DE3) cells was performed in M9 minimal media containing 0%, 30%, 50% or 70% D_2O, using cells that had not been adapted for growth in D_2O-containing media. For a second labeling experiment in a M9 medium with 70% D_2O/30% H_2O we used cells that had been adapted for growth in D_2O by a series of cultures grown successively to stationary phase in M9 media containing 0%, 30% and 50% D_2O. The following observations were readily apparent: First, the generation time during exponential growth increases with increasing D_2O content (Figure 2a). The absolute generation times were 1.05 ± 0.04 h for M9 in 100% H_2O, 1.14 ± 0.08 h, 1.26 ± 0.08 h and 1.50 ± 0.08 h for the media with 30%, 50% and 70% D_2O, where the generation times for adapted and non-adapted cells were identical within the accuracy of the measurements. Second, the final cell density in stationary phase is reduced at higher D_2O contents, and higher final cell densities were obtained with the pre-adapted cells (data not shown). No significant amounts of secreted metabolites could be detected in the growth medium at the end of the exponential growth phase, indicating that the glucose uptake is balanced with the biomass production and the generation of carbon dioxide.

Important insights were obtained from studies of the correlation of the level of intact multiple-carbon fragments from the carbon source molecules with the deuteration patterns of individual carbon sites in the amino acids. It was therefore essential to clarify the extent to which H↔D exchange occurred during hydrolysis of the cell protein. This information was obtained from studies of fractionally ^{13}C-labeled

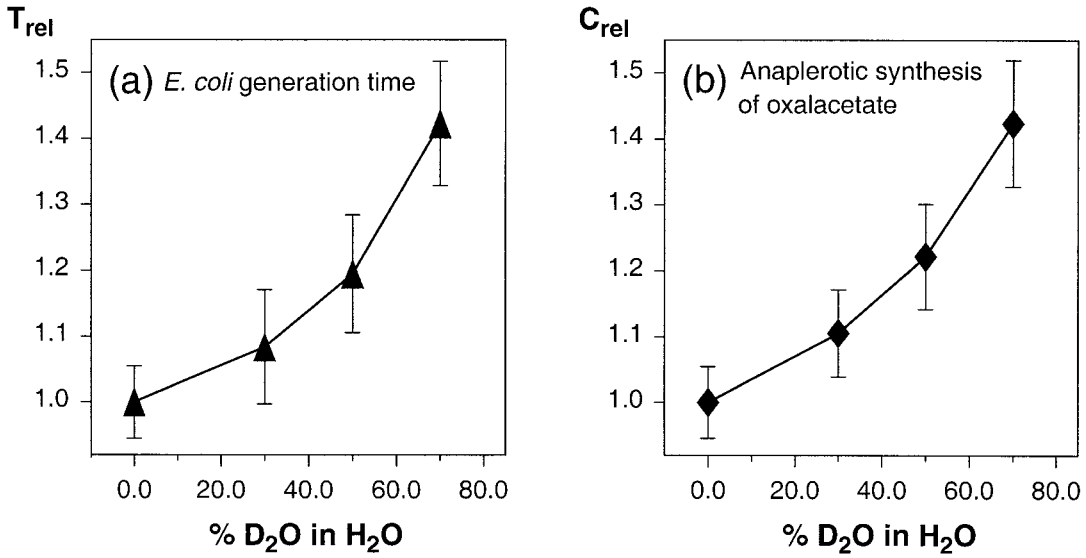

Figure 2. (a) Increase of the relative generation time, T_{rel} of *E. coli* BL21(DE3)pBR322 cells during exponential growth in M9 minimal medium with increasing concentrations of D_2O. (b) Increase of the fraction of oxalacetate (total pool) synthesized via anaplerotic carboxylation of phosphoenolpyruvate with increasing D_2O content of the nutrient medium, C_{rel}, as obtained from fractional ^{13}C-labeling experiments (Table 1). In (a) and (b) the values for 100% H_2O are arbitrarily set to 1.0, and the experimental errors indicated by the vertical bars for the relative values were calculated from the experimental error of the absolute values using the Gaussian law of error propagation.

biomass that had been harvested at the end of the exponential growth phase in M9 medium in H_2O and then hydrolysed in 6M deuterium chloride. The 2D [^{13}C,^{1}H]-HSQC spectra recorded with this preparation showed that H↔D exchange during hydrolysis was strictly limited to C^{β} of Asp, C^{γ} of Glu and C^{ϵ} of Tyr.

The relative abundances of intact carbon fragments from a single glucose molecule in the amino acids (*f* values; see Szyperski, 1995) were calculated from the analysis of the relative multiplet intensities in the ^{13}C-^{13}C scalar coupling fine structures observed in different types of [^{13}C,^{1}H]-correlation NMR spectra of the hydrolysed biomass (Figure 3). Analysis of the *f* values in terms of the patterns of intact carbon fragments in the metabolic intermediates from which the amino acids are synthesized was performed as described by Szyperski (1995). A fundamental result thus obtained is that the *f* values are in agreement with the standard biosynthesis pathways (Voet and Voet, 1995; Neidhardt et al., 1996), indicating that the topology of these pathways remains unchanged at elevated D_2O contents.

The ^{13}C scalar coupling fine structures for different deuterium isotopomers of the amino acids were individually resolved (Figure 3), and on this basis we found that for some of the proteinogenic amino acids the *f* values correlate with the deuteration at certain carbon atoms. This was generally observed for the cases where the metabolic precursor of the amino acid is synthesized via two alternative pathways (see Figure 3 in Szyperski, 1995), so that different ^{13}C isotopomers introduced through the alternative pathways correlate with different degrees of deuteration caused by these variant pathways (Figure 4). Provided that there is no H↔D exchange either on the biosynthetic route from the intermediate to the amino acid or during hydrolysis (see above), this correlation is preserved and can be studied through analysis of the amino acids (Figure 4). For the group of amino acids synthesized from oxalacetate (Asp, Thr and Met) the *f* values are correlated with the extent of deuteration at C^{β} and reveal distinct patterns of intact carbon fragments, which identify different metabolic origins for the individual C^{β} deuterium isotopomers (Figure 3). H or D at C^{α}, and for Thr also at C^{γ}, is introduced during the synthesis from oxalacetate (Voet and Voet, 1995), and therefore the *f* values at these carbon positions do not correlate with the extent of deuteration at the same carbon sites (Figure 4). Since H↔D exchange at Asp C^{β} occurs during hydrolysis in hydrochloric acid (see above), the Asp $C^{\beta}H_2$ isotopomer dominates and represents essentially the whole oxalacetate pool. The virtually complete H↔D exchange at

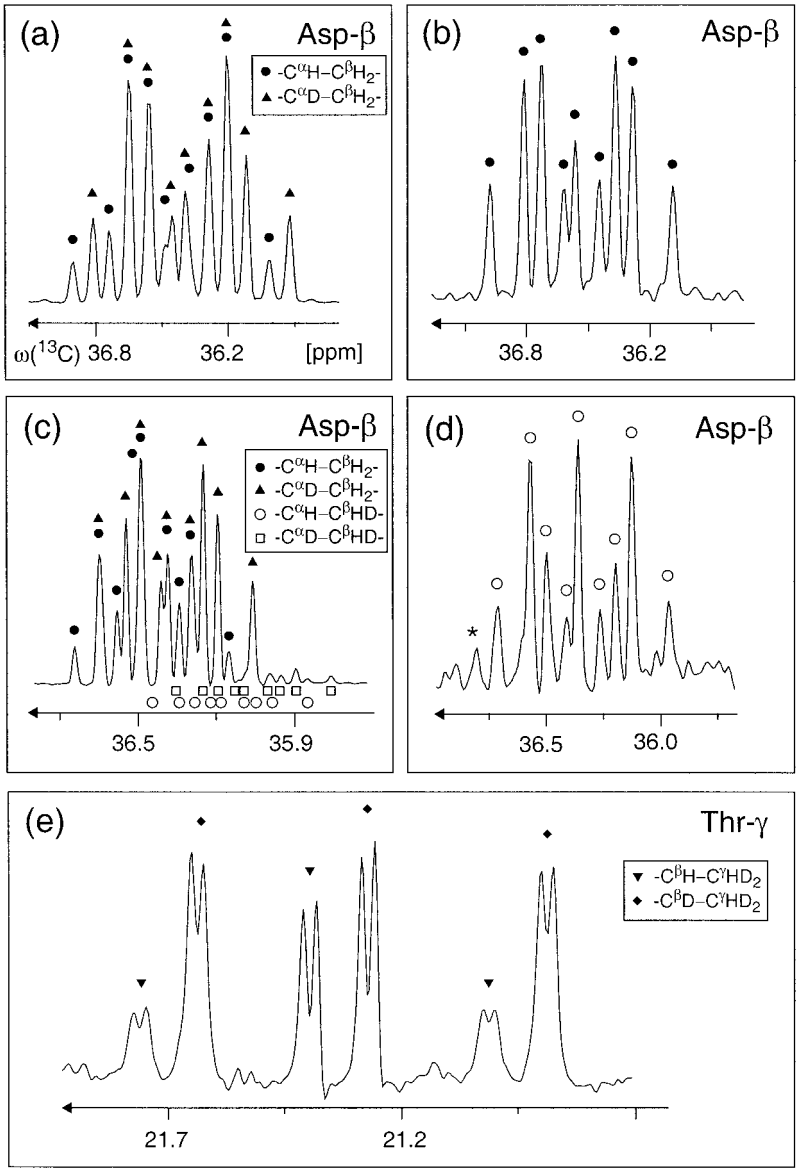

Figure 3. Illustration of the use of the different ^{13}C-^{1}H correlation experiments for observation of the ^{13}C-^{13}C scalar coupling fine structures of different aspartate and threonine deuterium isotopomers obtained from *E. coli* BL21(DE3) cells grown on a M9 medium in 70% D_2O/30% H_2O. All spectra were recorded with a Bruker DRX500 spectrometer at a ^{13}C resonance frequency of 125.8 MHz, except that (c) was recorded with a Bruker DRX750 spectrometer at a ^{13}C resonance frequency of 188.6 MHz. (a) Overlapping Asp-$^{13}C^{\beta}$ fine structures of the $C^{\alpha}H$-$C^{\beta}H_2$ and $C^{\alpha}D$-$C^{\beta}H_2$ isotopomers detected on H^{β} in a 2D [^{13}C,^{1}H]-HSQC spectrum. (b) Asp-$^{13}C^{\beta}$ fine structure of the $C^{\alpha}H$-$C^{\beta}H_2$ isotopomer detected on H^{α} in a 2D ^{1}H-TOCSY-relayed [^{13}C,^{1}H]-HSQC spectrum. (c) Asp-$^{13}C^{\beta}$ fine structures detected on H^{β} in a 2D [^{13}C,^{1}H]-HSQC spectrum recorded at a ^{1}H resonance frequency of 750 MHz. The $C^{\beta}H_2$ isotopomers dominate and the trace amounts of the $C^{\beta}HD$ isotopomers are also visible. (d) Resolved $^{13}C^{\beta}$ fine structure of the $C^{\alpha}H$-$C^{\beta}HD$ isotopomer detected on H^{α} in the refocused 2D ^{1}H-TOCSY-relayed [^{13}C,^{1}H]-HSQC spectrum tuned for selection of C-H groups. Note the differences in the relative multiplet intensities when compared to the $C^{\alpha}H$-$C^{\beta}H_2$ isotopomer in (b). The star denotes an impurity. (e) Resolved Thr-$^{13}C^{\gamma}$ fine structures of the $C^{\beta}D$-$C^{\gamma}HD_2$ and $C^{\beta}H$-$C^{\gamma}HD_2$ isotopomers in a 2D [^{13}C,^{1}H]-HSQC spectrum with J-scaling by a factor of 2.5. The three-bond deuterium isotope effect of C^{α}-D on the chemical shift of Thr-$^{13}C^{\gamma}$ causes additional doubling of the multiplet components (Hansen, 1988). A reduced degree of deuteration at Thr-$^{13}C^{\alpha}$ of about 50% is indicated, which presumably arises from the faster conversion of C^{α}-^{1}H phosphohomoserine by threonine synthase due to a primary isotope effect (Barclay et al., 1996). Note that the doublet components in the $C^{\beta}D$ isotopomer are more intense, which indicates a higher fraction of intact C^{β}-C^{γ} source fragments. In contrast, the relative multiplet intensities do not correlate with the extent of deuteration at C^{α}. The components of the multiplet structures originating from the different deuterium isotopomers are identified by symbols that are explained by the inserts in the panels (a), (c) and (e).

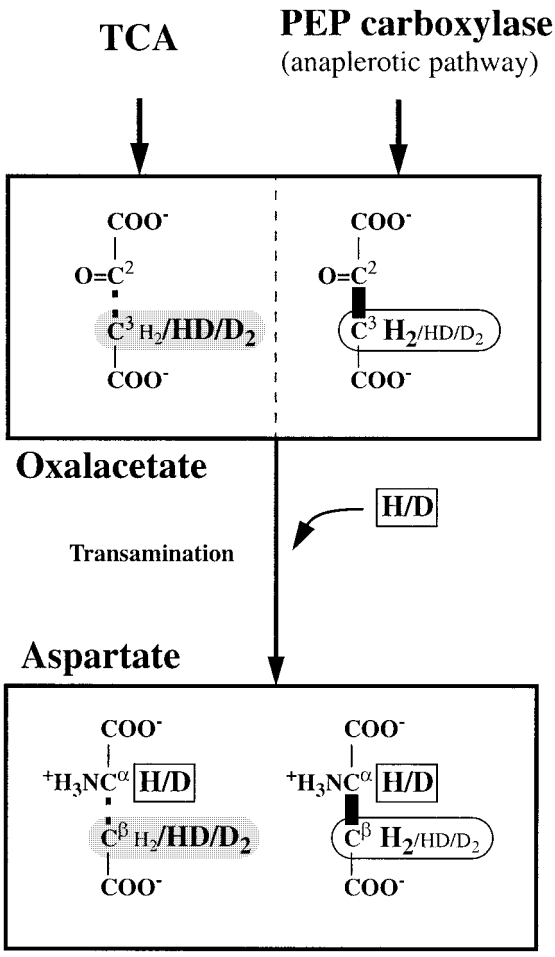

Figure 4. Correlation of the abundance of intact carbon fragments from the source glucose in aspartate with deuterium labeling after growth on an M9 medium in 70% D_2O/30% H_2O. Oxalacetate is synthesized via two alternative pathways, each of which may generate molecules that have different patterns of intact carbon fragments as well as different degrees of deuteration. Intact C_2-C_3 fragments in oxalacetate (thick line) arise exclusively from Pep via the anaplerotic pathway. Molecules deuterated at C^3 are preferentially generated via the TCA cycle, while the anaplerotic reaction introduces a larger fraction of fully protonated species (see text and Table 1). In the biosynthesis of Asp from oxalacetate via a transaminase no H↔D exchange occurs at C^β, while H or D are statistically introduced at C^α. As a consequence, the pattern of intact carbon fragments observed for Asp correlates with the deuteration of C^β but not with the deuteration of C^α, i.e., Asp C^βHD and Asp $C^\beta D_2$ exhibit a larger fraction of cleaved C^α-C^β connectivities than Asp $C^\beta H_2$. Note that observation of these labeling patterns in the present experiments is obtained from very weak signals for Asp C^βHD (Figure 3, c and d) because of the H↔D exchange at Asp C^β during hydrolysis (see text). Thick C-C bonds: intact carbon fragments originating from a single source molecule of glucose. Dotted C-C bonds: C-C connectivities newly formed during the biosynthesis. Thin C-C bonds: not specified here. PeP: phosphoenolpyruvate. TCA: tricarboxylic acid cycle.

Asp C^β during hydrolysis then enables accurate determination of the ratio of anaplerotic versus oxidative synthesis of oxalacetate in spite of the correlation between the *f* values and the extent of deuteration. Trace amounts of Asp C^βHD were detectable (Figure 3), whereby in the fine structures observed on H^α the two Asp C^βHD stereoisomers give identical spectra. These trace amounts of Asp C^β HD can be used to determine the *f* values for the pool of oxalacetate molecules that are deuterated at C^3. Moreover, oxalacetate that is not deuterated at C^3 can independently be qualitatively assessed via Thr. The correlation of deuteration at Thr C^β with the abundance of intact C^β-C^γ fragments is experimentally accessible through inspection of the C^γ fine structures of the C^βH-$C^\gamma HD_2$ and C^βD-$C^\gamma HD_2$ isotopomers. These fine structures can be neatly resolved in a 2D [^{13}C,^{1}H]-HSQC spectrum recorded with 2.5-fold J-scaling (Hosur, 1990; Willker et al., 1997) (Figure 3e). In principle, this analysis could be extended to the ^{13}C fine structures of Met, but these have not been sufficiently well resolved to allow determination of *f* values.

Correlations of the *f* values with the degree of deuteration prevail also for the amino acids derived from C_1-metabolism. For Ser, the relative abundance of intact C^α-C^β fragments correlates with the deuteration at C^β, and for Gly the *f* values correlate with the deuteration at C^α. For the amino acids synthesized from ribose-5-phosphate, erythrose-4-phosphate, phosphoenolpyruvate, pyruvate and acetyl-CoA, the *f* values do not correlate with the deuteration patterns and correspond to the values found for the preparations with M9 medium in H_2O. Similarly, the *f* values observed for the amino acids synthesized from 2-oxoglutarate do not vary with the degree of deuteration and correspond to the patterns of intact carbon fragments in the whole oxalacetate pool as assessed from Asp $C^\beta H_2$, and in acetyl-CoA as assessed from Leu C^α. This can be rationalized by the fact that 2-oxoglutarate is exclusively formed by irreversible condensation of oxalacetate with acetyl-CoA in the tricarboxylic acid cycle (TCA).

For a quantitative analysis of correlations between the extent of deuteration in metabolic intermediates and the abundance of intact two- and three-carbon fragments in the amino acids one also needs to account for possible deuterium isotope effects during the amino acid biosynthesis. For hydrogen atoms bound to carbons that are not involved in the formation or breakage of chemical bonds during biosynthesis, there are only small secondary isotope effects, which can

be neglected in the framework of the present study. For example, the deuteration of C^3 during transamination of oxalacetate into Asp is solely affected by a secondary isotope effect, so that the correlation between deuteration of C^3 and the *f* values inferred from the analysis of Asp C^β is not significantly affected by isotope effects. In contrast, inferences on isotopomers in oxalacetate derived from observations of Thr may be influenced by the primary isotope effects on the threonine synthase reaction (Barclay et al., 1996), and therefore the results derived from analysis of Thr are only valid as qualitative indications.

The evaluation of the relative abundances of intact carbon fragments in the pools of the eight principal intermediates that link primary metabolism to amino acid biosynthesis determines their metabolic origins and yields information on the active biochemical pathways and the flux ratios at several key points in central metabolism (Szyperski, 1995; Szyperski et al., 1996; Sauer et al., 1997). The flux ratios characterizing glycolysis and the pentose phosphate pathway were not measurably affected by the addition of D_2O (Table 1). In contrast, at higher D_2O contents the anaplerotic supply of the TCA cycle via carboxylation of phosphoenolpyruvate increased relative to the influx of acetyl-CoA (Figure 2b; Table 1), i.e., a larger fraction of the oxalacetate pool (as assessed from Asp $C^\beta H_2$) is synthesized via the anaplerotic reaction. Furthermore, the correlation of the patterns of intact carbon fragments in oxalacetate with the extent of deuteration at C^3 reveals different metabolic origins for the individual deuterium isotopomers in the metabolic network. Thr and Asp molecules deuterated at C^β (Thr $C^\beta D$ and the aforementioned trace amounts of residual Asp $C^\beta HD$) exhibit a lower fraction of intact C^α-C^β connectivities than Thr $C^\beta H$ or Asp $C^\beta H_2$ (Thr $C^\beta D$: 34%; Asp $C^\beta HD$: 26%; Thr $C^\beta H$: 59%; Asp $C^\beta H_2$: 48%). Consistently, Thr $C^\beta D$ displays a higher fraction of intact C^β-C^γ connectivities than Thr $C^\beta H$ (Thr $C^\beta D$: 58%; Thr $C^\beta H$: 32%), as is readily apparent from the more intense doublet component of the $C^\beta D$ isotopomer in the ^{13}C fine structures of Thr C^γ (Figure 3e). We conclude that oxalacetate deuterated at C^3 is preferentially generated via the TCA cycle (Table 1) while the anaplerotic reaction introduces a larger fraction of non-deuterated species via carboxylation of phosphoenolpyruvate. The difference between the *f* values of Thr $C^\beta D$ and Asp $C^\beta HD$ is presumably due to the aforementioned deuterium isotope effects on the threonine synthase reaction (Barclay et al., 1996).

The observations on the different metabolic origins of individual deuterium isotopomers of oxalacetate reveal that the metabolites in the TCA cycle are more highly deuterated than those in glycolysis. This can also be inferred from the analysis of Ser. The Ser $C^\beta H_2$ isotopomer clearly dominates at all D_2O contents of the medium, and it derives to a large extent directly from 3-phosphoglycerate since only a minor fraction has been reversibly interconverted to glycine and a C_1 unit via serine hydroxymethyltransferase (Table 1). This indicates in turn that C^3 of 3-phosphoglycerate must be highly protonated, since H or D at serine C^β is not introduced or exchanged on the biosynthesis route from 3-phosphoglycerate to Ser. The Ser $C^\beta HD$ isotopomer is present only in small amounts, and a higher fraction of this isotopomer derives from Gly and a C_1 unit (Table 1). The C_1 metabolic pathways generating glycine are also affected by the presence of D_2O. At all D_2O levels the Gly $C^\alpha HD$ isotopomer derives directly from the C'-C^α fragment of Ser via the serine hydroxymethyltransferase, whereas at high D_2O concentrations a significant fraction of the $C^\alpha H_2$ isotopomer arises from a different pathway, i.e., from CO_2 and a C_1 unit through the reversible glycine cleavage reaction. Alternatively, the threonine degradation pathway (Voet and Voet, 1995) may contribute to the generation of the Gly $C^\alpha H_2$ isotopomer at high D_2O contents.

Discussion

The dominant impression from the present study is that, in spite of the well-known deuterium isotope effects on enzyme functions and on cell physiology in general (see Introduction), the addition of D_2O to the medium under the presently chosen growth conditions causes only a change in the regulation of the TCA cycle (Table 1) and influences the C_1 metabolic pathways involving Ser and Gly. With regard to the production of D-labeled proteins for structural studies, no obvious key to improved production is readily apparent, for example, through the addition of one or several metabolites in deuterated form, or similar. It remains to be seen to what extent growth conditions of cell cultures in D_2O might be optimized based on the following conclusions from the present data.

The relative increase in the anaplerotic supply of the TCA cycle is correlated with an increase of the generation time (Figure 2). However, since the total biomass production rate is reduced at higher D_2O

levels, one might rather have anticipated that the anaplerotic supply of the TCA pathway is concomitantly decreased. The observed increase of anaplerosis thus suggests that, compared with glycolysis and the pentose phosphate pathway, the presence of D_2O represses the TCA cycle and respiration more strongly. Inhibition of the TCA cycle by D_2O would be consistent with the increase in generation time (Figure 2a), since D_2O may limit energy generation by the TCA and its production of precursors such as 2-oxoglutarate, which is an essential intermediate both for the synthesis of amino acids and for the nitrogen metabolism of the cell in general (Voet and Voet, 1995; Neidhardt et al., 1996). In vitro studies showed that several enzymes of the TCA cycle are indeed significantly inhibited by D_2O solvent effects as well as by deuterated substrates, in particular succinate dehydrogenase (Laser and Slater, 1960; Thomson and Klipfel, 1960), malate dehydrogenase (Thomson et al., 1962), isocitrate dehydrogenase (Coleman and Chu, 1969), fumarase (Thomson, 1960) and aconitase (Thomson et al., 1966; Thomson and Nance, 1969). We now observed for *E. coli* cells grown in D_2O-containing minimal media with protonated glucose as the carbon source that the TCA metabolites are more highly deuterated than those in glycolysis. D_2O inhibition may thus possibly limit the flux through the TCA cycle, and yield increased levels of acetyl-CoA since the pentose phosphate pathway and glycolysis appear to be much less affected. Since phosphoenolpyruvate carboxylase is activated by acetyl-CoA (Canovas and Kornberg, 1965), the excess glycolytic intermediates could then in part be diverted through the anaplerotic pathway.

Increased relative anaplerosis has recently also been observed in *E. coli* cells grown under nitrogen limitation (Sauer et al., 1999) when compared to cells grown under glucose limitation. In the nitrogen-limited case, there was extensive overflow metabolism, which was manifested by a marked increase in the specific glucose consumption rate as well as in the specific production rates of acetate and pyruvate, while the specific oxygen consumption and CO_2 evolution rates varied little between the two conditions, indicating that there are only minor changes in respiratory metabolism. The observed relative increase of anaplerosis during nitrogen-limited growth could thus also be due to diversion of excess glycolytic intermediates through the anaplerotic pathway.

It has previously been observed that the supply of the TCA cycle in *E. coli* cells depends markedly on the aeration of the culture, where a decreased contribution of anaplerosis under conditions of strong aeration would most probably be due to the increased TCA flux (Wüthrich et al., 1992; Szyperski, 1995). Given the evidence that cell growth in D_2O-containing media is in part affected by the inhibitory effect of D_2O on the TCA cycle, strong aeration should be assured during production of deuterium-labeled proteins in D_2O-containing media, in order to maximize the TCA flux and thus possibly increase the yield of protein.

Acknowledgements

We thank Marcel Emmerling for the analysis of the secreted metabolites in the growth media and M. Geier for the careful processing of the manuscript. Financial support was obtained from the Swiss Priority Program in Biotechnology.

References

Barclay, F., Chrystal, E. and Gani, D. (1996) J. Chem. Soc., Perkin Trans. 1, 683–689.

Bax, A. and Davis, D.G. (1985) *J. Magn. Reson.*, **65**, 355–360.

Bax, A. and Pochapsky, S. (1992) *J. Magn. Reson.*, **99**, 638–643.

Burum, D.P. and Ernst, R.R. (1980) *J. Magn. Reson.*, **39**, 163–168.

Canovas, J.L. and Kornberg, H.L. (1965) *Biochim. Biophys. Acta*, **96**, 169–172.

Cavanagh, J. and Rance, M. (1992) *J. Magn. Reson.*, **96**, 670–678.

Coleman, R.F. and Chu, R. (1969) *Biochem. Biophys. Res. Commun.*, **34**, 528–535.

DeMarco, A. and Wüthrich, K. (1976) *J. Magn. Reson.*, **24**, 201–204.

Fiaux, J., Andersson, C.I.J., Holmberg, N., Bülow, L., Kallio, P.T., Szyperski, T., Bailey, J.E. and Wüthrich, K. (1999) *J. Am. Chem. Soc.*, **121**, 1407–1408.

Gardner, K.H. and Kay, L.E. (1998) *Annu. Rev. Biophys. Biomol. Struct.*, **27**, 357–406.

Glaser, R. (1999) FCAL, version 2.3.0.

Hansen, P.E. (1988) *Prog. NMR Spectrosc.*, **20**, 207–255.

Hochuli, M., Patzelt, H., Oesterhelt, D., Wüthrich K. and Szyperski, T. (1999) *J. Bacteriol.*, **181**, 3226–3237.

Hosur, R.V. (1990) *Prog. NMR Spectrosc.*, **22**, 1–53.

Katz, J.J. and Crespi, H.L. (1970) In *Isotope Effects in Chemical Reactions* (Eds., Collins, C.J. and Bowman, N.S.), Van Nostrand Reinhold Company, New York, NY, pp. 286–363.

Laser, H. and Slater, E.C. (1960) *Nature*, **187**, 1115–1117.

LeMaster, D.M. (1994) *Prog. NMR Spectrosc.*, **26**, 371–419.

Marion, D., Ikura, M., Tschudin, R. and Bax, A. (1989) *J. Magn. Reson.*, **85**, 393–399.

Neidhardt, F.C., Curtiss, R., Ingraham, J.L., Liu, E.C.C., Low, K.B., Magasamik, B., Reznikoff, W.G., Riley, M., Schaechter, M. and Umbarger, H.E. (Eds.) (1996) *Escherichia coli and Salmonella typhimurium*, 2nd ed., American Society for Microbiology, Washington, DC.

Neri, D., Szyperski, T., Otting, G., Senn, H. and Wüthrich, K. (1989) *Biochemistry*, **28**, 7510–7516.

Otting, G. and Wüthrich, K. (1988) *J. Magn. Reson.*, **76**, 569–574.
Sambrook, S., Fritsch, E.F. and Maniatis, T. (1989) *Molecular Cloning: A Laboratory Manual*, 2nd ed., Cold Spring Harbor Laboratory Press, Cold Spring Harbor, NY.
Sauer, U., Hatzimanikatis, V., Bailey, J.E., Hochuli, M., Szyperski, T. and Wüthrich, K. (1997) *Nat. Biotechnol.*, **15**, 448–452.
Sauer, U., Lasko, D.R., Fiaux, J., Hochuli, M., Glaser, R., Szyperski, T., Wüthrich, K. and Bailey, J.E. (1999) *J. Bacteriol.*, **181**, 6679–6688.
Saur, W.K., Crespi, H.L., Halevi, E.A. and Katz, J.J. (1968) *Biochemistry*, **10**, 3529–3536.
Saur, W.K., Peterson, D.T., Halevi, E.A., Crespi, H.L. and Katz, J.J. (1968) *Biochemistry*, **10**, 3537–3546.
Schowen, R.L. (1977) In *Isotope Effects on Enzyme-catalysed Reactions* (Eds., Cleland, W.W., O'Leary, M.H. and Northrop, D.B.), University Park Press, Baltimore, MD, pp. 64–99.
Schowen, K.B. and Schowen, R.L. (1982) *Methods Enzymol.*, **87C**, 551–606.
Senn, H., Werner, B., Messerle, B.A., Weber, C., Traber, R. and Wüthrich, K. (1989) *FEBS Lett.*, **249**, 113–118.
Shaka, A.J., Barker, P.B. and Freeman, R. (1985) *J. Magn. Reson.*, **64**, 547–552.
Shaka, A.J., Keeler, J., Frenkiel, T. and Freeman, R. (1983) *J. Magn. Reson.*, **52**, 335–338.
Shaka, A.J., Lee, C.J. and Pines, A. (1988) *J. Magn. Reson.*, **77**, 274–293.
Studier, W.F., Rosenberg, A.H., Dunn, A.H. and Dunendorff, J.W. (1990) *Methods Enzymol.*, **185**, 60–89.
Szyperski, T. (1995) *Eur. J. Biochem.*, **232**, 433–448.
Szyperski, T. (1998) *Q. Rev. Biophys.*, **31**, 41–106.
Szyperski, T., Bailey, J.E. and Wüthrich, K. (1996) *Trends Biotechnol.*, **14**, 453–459.
Szyperski, T., Glaser, R.W., Hochuli, M., Fiaux, J., Sauer, U., Bailey, J.E. and Wüthrich, K. (1999) *Metabol. Eng.*, **1**, 189–197.
Szyperski, T., Neri, D., Leiting, B., Otting, G. and Wüthrich, K. (1992) *J. Biomol. NMR*, **2**, 323–334.
Thomson, J.F. (1960) *Arch. Biochim. Biophys.*, **90**, 1–6.
Thomson, J.F., Bray, D.A. and Bummert, J.J. (1962) *Biochem. Pharmacol.*, **11**, 943–948.
Thomson, J.F. and Klipfel, F.J. (1960) *Biochim. Biophys. Acta*, **44**, 72–77.
Thomson, J.F. and Nance, S.L. (1969) *Arch. Biochem. Biophys.*, **135**, 10–13.
Thomson, J.F., Nance, S.L., Bush, K.J. and Szczepanik, P.A. (1966) *Arch. Biochem. Biophys.*, **117**, 65–74.
Venters, R.A., Huang, C.C., Farmer, B.T., Trolard, R., Spicer, L.D. and Fierke, C.A. (1995) *J. Biomol. NMR*, **5**, 339–344.
Voet, D. and Voet, J.G. (1995) *Biochemistry*, 2nd ed., Wiley, New York, NY.
Wider, G. and Wüthrich, K. (1993) *J. Magn. Reson.*, **102**, 239–241.
Willker, W., Flögel, U. and Leibfritz, D. (1997) *J. Magn. Reson.*, **125**, 216–219.
Wüthrich, K., Szyperski, T., Leiting, B. and Otting, G. (1992) In *Frontiers and New Horizons in Amino Acid Research* (Proc. 1st Biennial International Conference on Amino Acid Research, Frontiers and Horizons, K. Takai, Ed.), Elsevier, Amsterdam, pp. 41–48.